

Consistency relation for R^p inflation

Hayato Motohashi

Kavli Institute for Cosmological Physics, The University of Chicago, Chicago, Illinois 60637, U.S.A.

(Dated: July 3, 2018)

We consider R^p inflation with $p \approx 2$, allowing small deviation from R^2 inflation. Using the inflaton potential in the Einstein frame, we construct a consistency relation between the scalar spectral index, the tensor-to-scalar ratio, as well as the running of the scalar spectral index, which will be useful to constrain a deviation from R^2 inflation in future observations.

I. INTRODUCTION

The first self-consistent model of inflation is R^2 inflation proposed by Starobinsky in 1980 [1], where R is the Ricci curvature. This model incorporates a graceful exit to the radiation-dominated stage via a period of reheating, where the standard model particles are created through the oscillatory decay of the inflaton, or dubbed the scalaron [2–4]. The predictions of R^2 inflation for the spectra of primordial density perturbations and gravitational waves remain in agreement with the most recent high-precision data of the cosmic microwave background (CMB) [5, 6]. In March 2014, BICEP2 announced the detection of B-mode polarization at degree angular scales in the CMB, and the amplitude of the tensor-to-scalar-ratio is as large as $r = 0.20^{+0.07}_{-0.05}$ [7], which is in tension with previous data as well as the prediction of R^2 inflation. However, it is still unclear if the signal is of primordial origin, due to an unknown amplitude of foreground dust emission [8]. In light of this, R^2 inflation is still consistent with the recent data and upcoming data may allow us to pin down the inflationary model of our universe.

In addition to inflation, the R^2 term play a different role in the context of $f(R)$ gravity for the late-time acceleration. By choosing a suitable functional form of $f(R)$, $f(R)$ gravity can mimic the expansion history of the concordance Λ CDM model without a cosmological constant [9–11]. Observationally, a key to distinguish $f(R)$ gravity from the Λ CDM model is the expansion history and the growth of the large-scale structure, which are conveniently parametrized by the equation-of-state parameter w for dark energy and the growth index γ , respectively, because both parameters remain constant in the Λ CDM model, namely, $w = -1$ and $\gamma = 0.55$, while they are dynamical in $f(R)$ gravity [9, 12–17]. In particular, it is interesting that $f(R)$ gravity allows a 1 eV sterile neutrino [18], whose existence has been suggested by recent neutrino oscillation experiments but is in tension with vanilla Λ CDM. However, the $f(R)$ models for the late-time acceleration suffer from singularity problems, where the scalaron mass and Ricci curvature diverge quickly in the past [11, 19–22]. These problems are solved if we add R^2 term [23]. The resultant combined $f(R)$ model incorporates inflation and the late-time acceleration. In the combined model, inflationary dynamics is still the same as R^2 inflation, while differences show up in reheating phase dominated by the kinetic energy of the scalaron [24], which enhances the tensor power spectrum [25].

The R^2 model is thus attractive in the sense that it is currently one of the leading candidates for inflation and it cures singularity problems when combined with $f(R)$ models for the late-time acceleration. Although it is simple and powerful, with progress in observational accuracy, we can test for further complexity. Similar to the generalization from a scale-invariant spectrum to a nonzero tilt, we may be forced to consider a small deviation from R^2 inflation. Specifically, tiny tensor-to-scalar ratio for R^2 inflation, namely, $r \simeq 0.003$ for 60 e-folds, motivates us to consider a deviation from R^2 inflation. We are poised to possibly obtain strong constraints on r from joint analysis of Planck and BICEP2 data, along with future experiments. It is therefore interesting to consider the possibility to generate larger value of r based on the R^2 model.

In order to establish a way to measure a deviation from R^2 inflation, we investigate R^p inflation in the present paper, where $p \approx 2$ and is not an integer, allowing small deviation from $p = 2$. The R^p Lagrangian was originally considered in the context of higher derivative theories [26, 27] and then applied to inflation [28, 29] (see also [30–32] for recent review), which provides a simple and economical generalization of R^2 inflation. Recently, R^p inflation has been focused in the context of the generation of large r . It has been emphasized that for p slightly smaller than 2, the tensor-to-scalar ratio can be enhanced relative to the original R^2 model [33] (see also [34]). A combined $f(R)$ model based on the R^p model has also been proposed [35]. Not only is it of phenomenological interest, the R^p action is also theoretically motivated because one-loop corrections to the R^2 action could give a correction to the power of the Ricci scalar [33, 36, 37]. A deformation of the R^2 action that mimics higher-loop corrections is considered in [38]. A relevance to Higgs inflation is considered in [39, 40].

However, its prediction to the scalar spectral index n_s , the tensor-to-scalar ratio r , as well as the running of the scalar spectral index $\alpha \equiv dn_s/d \ln k$ is not well formulated. In particular, some of the previous results provide different results for the prediction of n_s and r . Further, the running of the scalar spectral index in the model has not been discussed in the literature. The aim of the present paper is to resolve these issues and present a consistency relation

for R^p inflation by using the inflaton potential in the Einstein frame. We consider not only the scalar spectral index and the tensor-to-scalar ratio, but also the running of the scalar spectral index. We derive a handy expression for these inflationary observables, which will be useful to constrain a deviation from R^2 inflation in future observations.

The organization of the paper is as follows. In Sec. II, we explore the background dynamics of the inflationary expansion in R^p inflation. We write down the inflaton potential for general p in the Einstein frame and the slow-roll parameters in terms of the derivatives of the potential. In Sec. III, we derive a consistency relation between the inflationary observables, with which we can constrain the model. We conclude in Sec. IV. Throughout the paper, we will work in natural units where $c = 1$, and the metric signature is $(-+++)$.

II. R^p INFLATION

Let us start with a general $f(R)$ and write down equations of motion in the Einstein frame. We consider

$$S = \int d^4x \sqrt{-g} \frac{M_{\text{Pl}}^2}{2} f(R), \quad (1)$$

where $M_{\text{Pl}} \equiv (8\pi G)^{-1/2}$ is the reduced Planck mass. By using the conformal transformation $g_{\mu\nu}^E \equiv F(R)g_{\mu\nu}$ with defining the scalaron field ϕ by $F(R) \equiv f'(R) \equiv e^{\sqrt{\frac{2}{3}}\frac{\phi}{M_{\text{Pl}}}}$, we can recast the action as

$$S = \int d^4x \sqrt{-g_E} \left[\frac{M_{\text{Pl}}^2}{2} R_E - \frac{1}{2} g_E^{\mu\nu} \partial_\mu \phi \partial_\nu \phi - V(\phi) \right], \quad (2)$$

where the potential is given by

$$V(\phi) = \frac{M_{\text{Pl}}^2}{2} \frac{\chi F(\chi) - f(\chi)}{F(\chi)^2}. \quad (3)$$

Here, $\chi = \chi(\phi)$ is a solution for $F(\chi) = e^{\sqrt{\frac{2}{3}}\frac{\phi}{M_{\text{Pl}}}}$, and thus $f(\chi)$ and $F(\chi)$ are determined for each ϕ . The time and the scale factor in the Jordan frame and Einstein frame relate through

$$dt_E = \sqrt{F} dt, \quad a_E = \sqrt{F} a, \quad (4)$$

and thus the Hubble parameter in the Einstein frame is given by

$$H_E = \frac{H}{\sqrt{F}} \left(1 + \frac{\dot{F}}{2HF} \right), \quad (5)$$

where a dot implies the derivative with respect to the time t in the Jordan frame. The Einstein equation reads

$$3M_{\text{Pl}}^2 H_E^2 = \frac{1}{2} \left(\frac{d\phi}{dt_E} \right)^2 + V, \quad (6)$$

$$-2M_{\text{Pl}}^2 \frac{dH_E}{dt_E} = \left(\frac{d\phi}{dt_E} \right)^2, \quad (7)$$

and the equation of motion for the scalaron is given by

$$\frac{d^2\phi}{dt_E^2} + 3H_E \frac{d\phi}{dt_E} + V_\phi = 0, \quad (8)$$

where $V_\phi \equiv \partial V / \partial \phi$.

For the rest of the paper, we focus on the following model:

$$f(R) = R + \lambda R^p. \quad (9)$$

The parameter p is not necessarily an integer in general, and λ has mass dimension $(2-p)$. In this model, the potential (3) can be explicitly written in terms of ϕ as

$$V(\phi) = V_0 e^{-2\sqrt{\frac{2}{3}}\frac{\phi}{M_{\text{Pl}}}} \left(e^{\sqrt{\frac{2}{3}}\frac{\phi}{M_{\text{Pl}}}} - 1 \right)^{\frac{p}{p-1}} \quad (10)$$

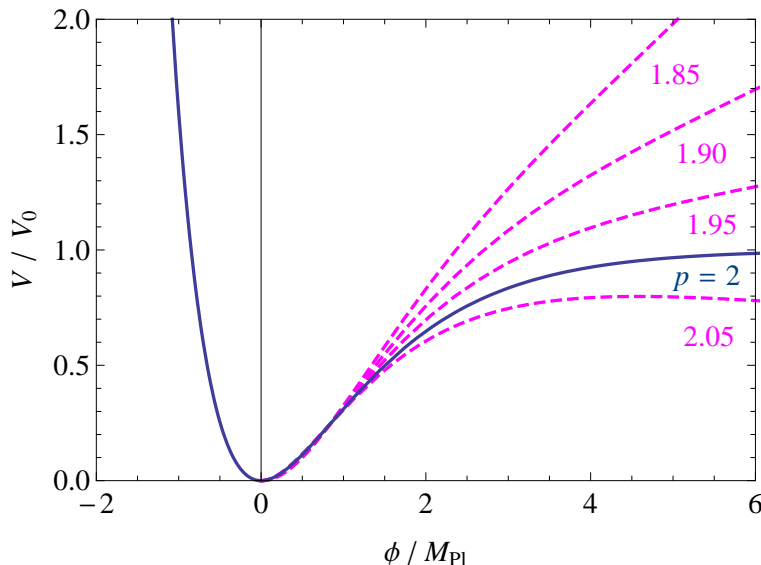


Figure 1. Potential for R^p inflation with $p = 2$ (blue solid), and 1.85, 1.90, 1.95, 2.05 (magenta dashed).

with $V_0 \equiv \frac{M_{\text{Pl}}^2}{2}(p-1)p^{p/(1-p)}\lambda^{1/(1-p)}$. Note that for $p = 2$ and $\lambda = 1/(6M^2)$, the potential (10) recovers the potential for R^2 inflation:

$$V(\phi) = \frac{3}{4}M^2M_{\text{Pl}}^2(1 - e^{-\sqrt{\frac{2}{3}}\frac{\phi}{M_{\text{Pl}}}})^2, \quad (11)$$

where the energy scale is normalized as $M \simeq 10^{13}$ GeV from the amplitude of observed power spectrum for the primordial perturbations.

In Fig. 1, we present the potential (10) for various p around $p = 2$. The scalaron rolls slowly on the potential at $\phi > 0$, and leads the inflationary expansion. While the potential for $p = 2$ asymptotically approaches to a constant value V_0 for large ϕ , the potential for $p \lesssim 2$ continuously grows. Therefore, the potential for $p \lesssim 2$ is steeper than $p = 2$, and this leads to larger tensor-to-scalar ratio relative to R^2 inflation, as we shall see later. For $p > 2$, the potential (10) has a maximum at $\phi = M_{\text{Pl}}\sqrt{\frac{3}{2}}\ln\left[\frac{2(p-1)}{p-2}\right] \equiv \phi_m$ and approaches to 0 for large ϕ . For instance, $\phi_m/M_{\text{Pl}} \simeq 4.58$ for $p = 2.05$. Therefore, inflation can take place at either of $0 < \phi < \phi_m$ or $\phi > \phi_m$. We are interested in the former case to see a deviation from R^2 inflation, and do not consider the latter case, which leads to a completely different scenario from R^2 inflation.

We define the slow-roll parameters for the potential in the Einstein frame as

$$\epsilon \equiv \frac{M_{\text{Pl}}^2}{2} \left(\frac{V_\phi}{V} \right)^2, \quad \eta \equiv M_{\text{Pl}}^2 \frac{V_{\phi\phi}}{V}, \quad \xi \equiv M_{\text{Pl}}^4 \frac{V_\phi V_{\phi\phi\phi}}{V^2}. \quad (12)$$

Under the slow roll approximation, (6) – (8) read

$$H_E \simeq \frac{\sqrt{V}}{\sqrt{3}M_{\text{Pl}}}, \quad \frac{dH_E}{dt_E} \simeq -\frac{V_\phi^2}{6V}, \quad \frac{d\phi}{dt_E} \simeq -\frac{M_{\text{Pl}}V_\phi}{\sqrt{3V}}. \quad (13)$$

During slow-roll regime, the scale factor in the Einstein frame undergoes a quasi-de Sitter expansion. From $|\dot{F}/(HF)| \simeq 2\sqrt{\epsilon/3} \ll 1$, F remains approximately constant during the slow-roll regime. Hence, from (4) the scale factor and time in the Einstein frame are identical to those in the Jordan frame up to a constant factor. Consequently, the quasi-de Sitter expansion takes place in both frame. The number of e-folds between an initial time t_{Ei} and t_E is given by

$$N_E \equiv \int_{t_{Ei}}^{t_E} H_E dt_E \simeq \frac{1}{M_{\text{Pl}}^2} \int_{\phi}^{\phi_i} \frac{V}{V_\phi} d\phi. \quad (14)$$

Note that from (4) and (5) $H_E dt_E = H dt [1 + \dot{F}/(2HF)] \simeq H dt$ during the slow-roll regime and therefore $N_E \simeq N$. Armed with these equivalences between quantities in the Jordan frame and Einstein frame during inflation, we omit the subscript E for the following and continue to explore the inflationary dynamics in the Einstein frame.

Before proceeding to detailed analysis for $p = 2$ and general p , let us here clarify the differences of the potential in the previous works. In [39], the authors consider R^p model (9) at first but eventually investigate the potential $V \propto (1 - \gamma e^{-\beta\phi})$ with β and γ as free parameters. This potential is obviously different from the potential (10) in R^p inflation because their potential approaches constant for large ϕ . They show that $\epsilon \ll |\eta|$ always holds, and n_s depends only on e-folds while r depends on the model parameters and e-folds. As we shall see below, these points are incompatible with R^p inflation.

In [40], the authors also start from R^p model (9) but arrive the potential $V \propto e^{\frac{2-p}{p-1}\sqrt{\frac{2}{3}}\frac{\phi}{M_{\text{Pl}}}}$, assuming $\phi/M_{\text{Pl}} \gg \sqrt{3/2} \simeq 1.22$. However, as we shall see, a field value which we are interested in is the same order of 1.22. In particular, their approximation breaks down as $p \rightarrow 2$, because the field value of our interest becomes closer to 1.22. Actually, their n_s and r does not recover R^2 inflation. Therefore, we cannot use their result if we want to consider small deviation from R^2 inflation.

Thus, although both works are motivated by R^p inflation, they did not investigate R^p inflation itself. Rather, they investigated the potential $V \propto (1 - \gamma e^{-\beta\phi})$ and $V \propto e^{\frac{2-p}{p-1}\sqrt{\frac{2}{3}}\frac{\phi}{M_{\text{Pl}}}}$, respectively, both of which cannot be used as an asymptotic form of the potential (10) of R^p inflation. On the other hand, our analysis is based on the potential (10) without any approximation.

A. $p = 2$

First, let us focus on the case with $p = 2$. The slow-roll parameters (12) for the potential (11) are given by

$$\begin{aligned}\epsilon &= \frac{4}{3(e^{\sqrt{\frac{2}{3}}\frac{\phi}{M_{\text{Pl}}}} - 1)^2}, \\ \eta &= -\frac{4(e^{\sqrt{\frac{2}{3}}\frac{\phi}{M_{\text{Pl}}}} - 2)}{3(e^{\sqrt{\frac{2}{3}}\frac{\phi}{M_{\text{Pl}}}} - 1)^2}, \\ \xi &= \frac{16(e^{\sqrt{\frac{2}{3}}\frac{\phi}{M_{\text{Pl}}}} - 4)}{9(e^{\sqrt{\frac{2}{3}}\frac{\phi}{M_{\text{Pl}}}} - 1)^3}.\end{aligned}\tag{15}$$

Thus the slow-roll parameters relate each other through ϕ , and we can derive the following relation between them:

$$\begin{aligned}\eta &= -\frac{2\sqrt{\epsilon}}{\sqrt{3}} + \epsilon, \\ \xi &= \frac{4}{3}\epsilon - 2\sqrt{3}\epsilon^{3/2}.\end{aligned}\tag{16}$$

Note that these relations are derived by only using the form of the potential. They hold exactly, regardless of the appearance of the slow-roll parameters. As we shall see later, it is when we convert these relations into a consistency relation between inflationary observables that we need the slow-roll approximation.

For $\phi > M_{\text{Pl}}$, the slow roll parameters are suppressed as $\epsilon, \xi \sim e^{-2\sqrt{\frac{2}{3}}\frac{\phi}{M_{\text{Pl}}}}$, and $|\eta| \sim e^{-\sqrt{\frac{2}{3}}\frac{\phi}{M_{\text{Pl}}}}$. It is worthwhile to note that the hierarchy between the slow-roll parameters is not $1 \gg \epsilon \sim |\eta| \gg \xi$ like ϕ^2 inflation, but $1 \gg |\eta| \gg \epsilon \sim \xi$, which leads to a tiny tensor-to-scalar ratio.

If we define the end of inflation by $\epsilon = 1$, a field value at the end of inflation ϕ_f is given by $\phi_f/M_{\text{Pl}} \simeq 0.940$. From (14), we obtain the e-folds between ϕ_i and ϕ as

$$N(\phi) = \frac{3}{4} \left(e^{\sqrt{\frac{2}{3}}\frac{\phi_i}{M_{\text{Pl}}}} - e^{\sqrt{\frac{2}{3}}\frac{\phi}{M_{\text{Pl}}}} \right),\tag{17}$$

where we neglect a linear term of $(\phi - \phi_i)$, which gives a few percent correction. We can solve this equation for ϕ ,

$$\frac{\phi(N)}{M_{\text{Pl}}} = \sqrt{\frac{3}{2}} \ln \left(e^{\sqrt{\frac{2}{3}}\frac{\phi_i}{M_{\text{Pl}}}} - \frac{4}{3}N \right),\tag{18}$$

and using the slow-roll equation (13) with the potential (11), the Hubble parameter is given by

$$\frac{H(N)}{\sqrt{V_0}/M_{\text{Pl}}} = \frac{1}{\sqrt{3}} \left[1 - \left(e^{\sqrt{\frac{2}{3}}\frac{\phi_i}{M_{\text{Pl}}}} - \frac{4}{3}N \right)^{-1} \right],\tag{19}$$

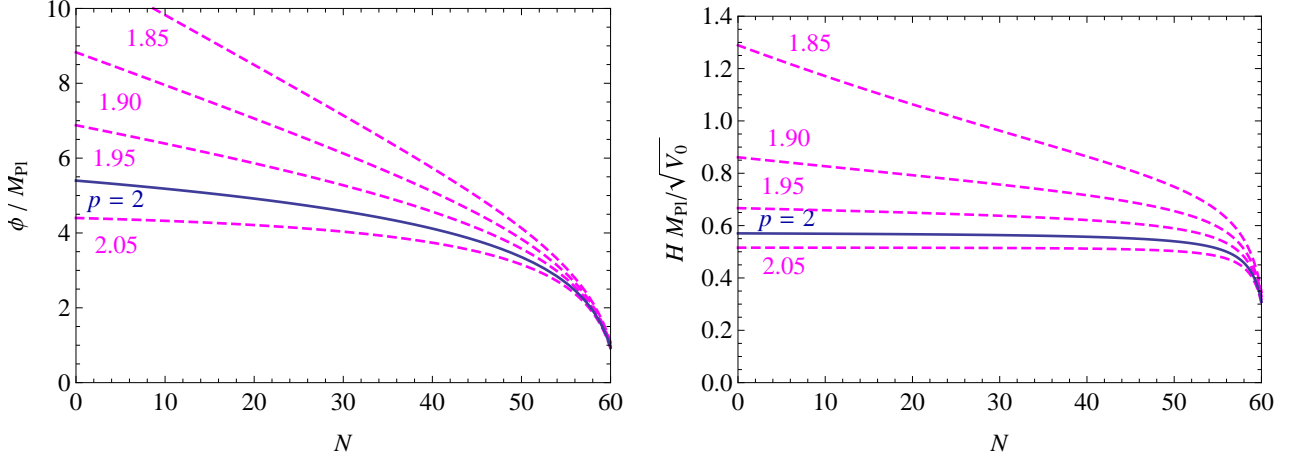


Figure 2. Time evolution of the scalaron ϕ and the Hubble parameter H for $p = 2$ (blue solid), and 1.85, 1.90, 1.95, 2.05 (magenta dashed).

which are presented as a blue solid line in Fig. 2.

If we require the total e-folds $N_k \equiv N(\phi_f) = 60$, we obtain $\phi_i / M_{\text{Pl}} \simeq 5.40$. Therefore, $N_k \simeq \frac{3}{4} e^{\sqrt{\frac{2}{3}} \frac{\phi_i}{M_{\text{Pl}}}}$, and at the leading order of N_k , the slow roll parameters (15) at $\phi \simeq \phi_i$ are expressed as

$$\epsilon = \frac{3}{4N_k^2}, \quad \eta = -\frac{1}{N_k}, \quad \xi = \frac{1}{N_k^2}. \quad (20)$$

B. $p \approx 2$

We proceed to a general case with $p \approx 2$. The slow-roll parameters (12) are given by

$$\begin{aligned} \epsilon &= \frac{[(2-p)F + 2(p-1)]^2}{3(p-1)^2(F-1)^2}, \\ \eta &= \frac{2[(2-p)^2F^2 - (p-1)(5p-8)F + 4(p-1)^2]}{3(p-1)^2(F-1)^2}, \\ \xi &= \frac{4[(2-p)F + 2(p-1)][(2-p)^3F^3 + (p-1)(2p-3)(5p-8)F^2 - (p-1)^2(17p-24)F + 8(p-1)^3]}{9(p-1)^4(F-1)^4}, \end{aligned} \quad (21)$$

where $F \equiv e^{\sqrt{\frac{2}{3}} \frac{\phi}{M_{\text{Pl}}}}$ as we defined the above. We can confirm that For $p = 2$, (21) reproduces (15). We can erase F from these equations and obtain

$$\begin{aligned} -4(2-p) + 2(3p-4)\sqrt{3}\epsilon - 6\epsilon + 3p\eta &= 0, \\ -2(2-p)(3p-4)\sqrt{3}\epsilon + 3(7p^2 - 24p + 24)\epsilon - 9\sqrt{3}(3p-4)\epsilon^{3/2} + 9(2-p)\epsilon^2 - \frac{9}{4}p^2\xi &= 0. \end{aligned} \quad (22)$$

Again, these relations hold without the slow-roll approximation.

The field value at the end of inflation $\epsilon = 1$ is given by

$$\frac{\phi_f}{M_{\text{Pl}}} = \sqrt{\frac{3}{2}} \ln \left[\frac{(2 + \sqrt{3})(p-1)}{(1 + \sqrt{3})p - (2 + \sqrt{3})} \right]. \quad (23)$$

For instance, $\phi_f / M_{\text{Pl}} \simeq 0.907, 0.978, 1.02, 1.07$ for $p = 2.05, 1.95, 1.90, 1.85$, respectively.

The number of e-folds between ϕ_i and ϕ given by (14) reads

$$N(\phi) = \frac{3p}{4(2-p)} \ln \left[\frac{(2-p)e^{\sqrt{\frac{2}{3}} \frac{\phi_i}{M_{\text{Pl}}}} + 2(p-1)}{(2-p)e^{\sqrt{\frac{2}{3}} \frac{\phi}{M_{\text{Pl}}}} + 2(p-1)} \right]. \quad (24)$$

Then we obtain

$$\frac{\phi(N)}{M_{\text{Pl}}} = \sqrt{\frac{3}{2}} \ln \left[E^{-1} \left(e^{\sqrt{\frac{2}{3}} \frac{\phi_i}{M_{\text{Pl}}}} + \frac{2(p-1)}{2-p} \right) - \frac{2(p-1)}{2-p} \right]. \quad (25)$$

From (13), the Hubble parameter is given by

$$\frac{H(N)}{\sqrt{V_0}/M_{\text{Pl}}} = \frac{1}{\sqrt{3}} \left[E^{-1} \left(e^{\sqrt{\frac{2}{3}} \frac{\phi_i}{M_{\text{Pl}}}} + \frac{2(p-1)}{2-p} \right) - \frac{p}{2-p} \right]^{\frac{p}{2(p-1)}} \left[E^{-1} \left(e^{\sqrt{\frac{2}{3}} \frac{\phi_i}{M_{\text{Pl}}}} + \frac{2(p-1)}{2-p} \right) - \frac{2(p-1)}{2-p} \right]^{-1}, \quad (26)$$

where $E(N) \equiv e^{4(2-p)N/(3p)}$. We present the time evolution of the scalaron and the Hubble parameter for $p = 2.05, 1.95, 1.90, 1.85$ by magenta dashed lines in Fig. 2. As expected, the scalaron rolls down faster for $p \lesssim 2$.

By setting $N_k \equiv N(\phi_f) = 60$, we obtain

$$\frac{\phi_i}{M_{\text{Pl}}} = \sqrt{\frac{3}{2}} \ln \left[E_k \left(e^{\sqrt{\frac{2}{3}} \frac{\phi_f}{M_{\text{Pl}}}} + \frac{2(p-1)}{2-p} \right) - \frac{2(p-1)}{2-p} \right], \quad (27)$$

where $E_k \equiv e^{4(2-p)N_k/(3p)}$. For instance, $\phi_i/M_{\text{Pl}} \simeq 4.40, 6.88, 8.83, 11.2$ for $p = 2.05, 1.95, 1.90, 1.85$, respectively. Therefore, for N_k we can neglect the contribution from ϕ_f and end up with

$$N_k \simeq \frac{3p}{4(2-p)} \ln \left[\frac{(2-p)}{2(p-1)} e^{\sqrt{\frac{2}{3}} \frac{\phi_i}{M_{\text{Pl}}}} + 1 \right]. \quad (28)$$

By taking the limit of $p \rightarrow 2$, we recover $N_k = \frac{3}{4} e^{\sqrt{\frac{2}{3}} \frac{\phi_i}{M_{\text{Pl}}}}$.

By substituting $F = 2(E_k - 1)(p - 1)/(2 - p)$, we obtain the slow-roll parameters (21) at $\phi \simeq \phi_i$ as

$$\begin{aligned} \epsilon &= \frac{4E_k^2(2-p)^2}{3[2(p-1)E_k - p]^2}, \\ \eta &= \frac{4(2-p)[2(2-p)E_k^2 - pE_k + p]}{3[2(p-1)E_k - p]^2}, \\ \xi &= \frac{16E_k(2-p)^2[4(2-p)^2E_k^3 + 2p(4p-7)E_k^2 - p(11p-18)E_k + p(3p-4)]}{9[2(p-1)E_k - p]^4}. \end{aligned} \quad (29)$$

Taking the limit $p \rightarrow 2$, we can recover the results in R^2 inflation.

In R^2 inflation, the hierarchy between the slow-roll parameters is $|\eta| \gg \epsilon \sim \xi$. However, it is not the case for R^p inflation with $p \neq 2$. The left panel of Fig. 3 exhibits the slow roll parameters (29) for $p \approx 2$ with $N_k = 60$ and 50 . Blue solid, magenta dashed, and green dot-dashed lines are ϵ , $|\eta|$, and ξ , respectively. Thick lines are for $N_k = 60$, while thin lines are for $N_k = 50$. Note that η flips its sign at $p \simeq 1.94$ for $N_k = 60$ ($p \simeq 1.93$ for $N_k = 50$): $\eta > 0$ for $p \lesssim 1.94$, and $\eta < 0$ for $p \gtrsim 1.94$. Now the hierarchy between the slow-roll parameters for $p \approx 2$ obviously varies from $|\eta| \gg \epsilon \sim \xi$ for $p = 2$. However, we note that ξ is always subleading. Therefore, for the following, we treat ϵ and η as the first order quantities, and ξ as the second order quantity.

III. CONSISTENCY RELATION

Now we want to relate the slow-roll parameters to the inflationary observables. Since the comoving curvature perturbation and the tensor perturbation are invariant under the conformal transformation [41, 42], we can make use of the slow-roll parameters obtained from the inflaton potential in the Einstein frame to evaluate the scalar spectral index n_s , its running $\alpha \equiv dn_s/d \ln k$, and the tensor-to-scalar ratio r . Up to the leading order of the slow-roll parameters, the inflationary observables can be written as

$$\begin{aligned} n_s - 1 &= -6\epsilon + 2\eta, \\ r &= 16\epsilon, \\ \alpha &= 16\epsilon\eta - 24\epsilon^2 - 2\xi. \end{aligned} \quad (30)$$

Let us remind that ξ is treated as the second order quantity here. This treatment is valid for R^p inflation and is also often implicitly assumed in the literature, but it is not necessarily always the case. For general case, where ξ can be comparable to ϵ and $|\eta|$, we need more careful treatment [43].

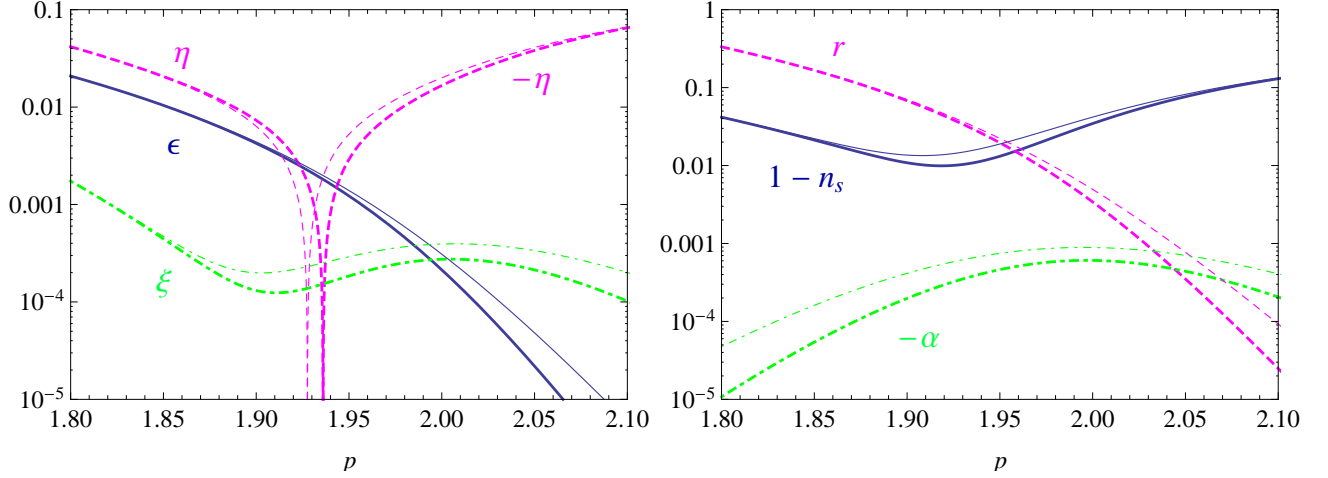


Figure 3. Left: Slow roll parameters, ϵ (blue solid), $|\eta|$ (magenta dashed), and ξ (green dot-dashed). Right: Inflationary observables, $1 - n_s$ (blue solid), r (magenta dashed), and $-\alpha$ (green dot-dashed). The thick lines and thin lines are for $N_k = 60$ and 50 , respectively.

A. $p = 2$

For $p = 2$, we can immediately write down (30) in terms of N_k by the virtue of (20). Up to the leading order of N_k^{-1} , we obtain

$$n_s - 1 = -\frac{2}{N_k}, \quad r = \frac{12}{N_k^2}, \quad \alpha = -\frac{2}{N_k^2}. \quad (31)$$

Thus the consistency relation is given by

$$n_s - 1 = -\sqrt{\frac{r}{3}}, \quad \alpha = -\frac{r}{6}. \quad (32)$$

Equivalently, we can derive the above relation using (16) and (30).

B. $p \approx 2$

For general p , by substituting (29) into (30), we obtain

$$\begin{aligned} n_s - 1 &= -\frac{8(2-p)[(2-p)E_k^2 + p(E_k - 1)]}{3[2(p-1)E_k - p]^2}, \\ r &= \frac{64E_k^2(2-p)^2}{3[2(p-1)E_k - p]^2}, \\ \alpha &= -\frac{32p(2-p)^2E_k(E_k - 1)(2E_k - 3p + 4)}{9[2(p-1)E_k - p]^4}. \end{aligned} \quad (33)$$

Thus, n_s , r , and α are related through the parameter $E_k = e^{4(2-p)N_k/(3p)}$. We can recover (31) if we take the limit $p \rightarrow 2$ in (33). By erasing E_k , we can obtain the consistency relation as

$$\begin{aligned} n_s - 1 &= -\frac{(3p-4)}{\sqrt{3}p}\sqrt{r} - \frac{3p-2}{8p}r + \frac{8(2-p)}{3p}, \\ \alpha &= \frac{4(2-p)(3p-4)}{3\sqrt{3}p^2}\sqrt{r} - \frac{15p^2 - 40p + 24}{6p^2}r - \frac{(3p-4)(4p-3)}{8\sqrt{3}p^2}r^{3/2} - \frac{(p-1)(3p-2)}{32p^2}r^2. \end{aligned} \quad (34)$$

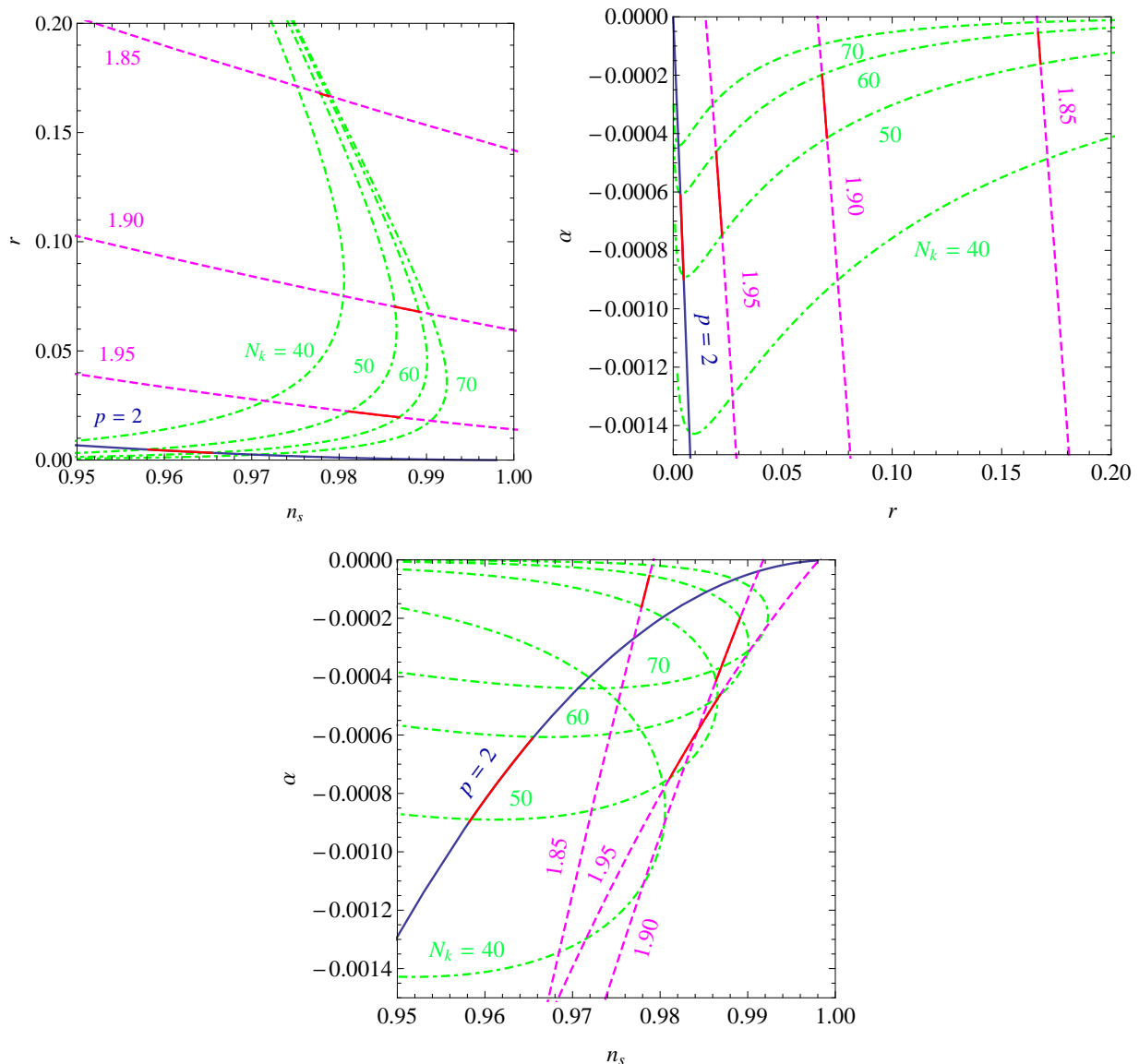


Figure 4. Scalar spectral index n_s , its running α , and tensor-to-scalar ratio r for $p = 2$ (solid blue), and 1.95, 1.90, 1.85 (magenta dashed), where e-folds between $N_k = 50$ and 60 are highlighted (red solid). Lines for fixed e-folds $N_k = 40, 50, 60, 70$ (green dot-dashed) are also shown.

In the right panel of Fig. 3, we present the scalar spectral index, its running, and the tensor-to-scalar ratio for $p \approx 2$ with $N_k = 60$ and 50. Blue solid, magenta dashed, green dot-dashed lines are $(1 - n_s)$, r , $-\alpha$, respectively, and thick and thin lines represent $N_k = 60$ and 50, respectively. We see that the scalar spectral index takes its maximum value $\simeq 0.99$ at $p \simeq 1.92$ and thus R^p inflation describe only red-tilted spectrum. For $p < 1.8$ or $p > 2$, we have $n_s < 0.96$. On the other hand, the tensor-to-scalar ratio increases as p decreases. Actually, r exceeds 0.1 and 0.2 at $p \simeq 1.88$ and $p \simeq 1.84$, respectively, for $N_k = 60$. As for the running of the scalar spectral index, α is always negative. Its amplitude takes the maximum value $\simeq 10^{-3}$ at $p \simeq 2$.

Using (33) or (34), we can explicitly draw the consistency relation between the inflationary observables as presented in Fig. 4. Blue solid lines represent $p = 2$, and magenta dashed lines represent $p = 1.95, 1.90, 1.85$. We also show lines for fixed e-folds N_k by green dot-dashed lines. We highlighted lines for fixed p with e-folds $50 < N_k < 60$. In particular, it is interesting that the scalar spectral index n_s is sensitive for a deviation from $p = 2$. The panel for (n_s, r) captures this property. For $1.8 < p < 2$, the spectral index varies as $0.96 \lesssim n_s \lesssim 0.99$ but is always larger than 0.96 for $N_k = 60$. For $p \gtrsim 1.95$, the spectral index is very sensitive for p . Therefore, the parameter region $p \gtrsim 1.95$ is solely constrained by n_s .

We are also interested in how future constraint on r tests the model. From the panel for (n_s, r) in Fig. 4, we note that for $N_k = 60$ small tensor-to-scalar ratio with $r \leq 0.05$ requires $1.92 \lesssim p \leq 2$ and $0.96 \lesssim n_s \lesssim 0.99$. For large r with $0.05 \leq r \leq 0.1$, p should be $1.88 \lesssim p \lesssim 1.92$ and n_s needs to be within $0.98 \lesssim n_s \lesssim 0.99$. On the other hand, for fixed $n_s = 0.96$, $r = 0.05$ and 0.1 require $(p, N_k) \simeq (1.93, 30)$ and $(1.9, 27)$, respectively.

From the panel for (r, α) in Fig. 4, we can explicitly see that a deviation from $p = 2$ suppresses α , while r is enhanced. This property is also useful to test R^p inflation. We can constrain p with an order 10^{-4} accuracy for α . The panel for (n_s, α) in Fig. 4 shows that it is difficult for this combination is to constrain p because the lines are overlapping and thus there is a degeneracy between parameters. Therefore, in order to constrain R^p inflation, it is important to measure both the scalar and the tensor spectra, namely, the combination of (n_s, r) or (r, α) would constrain the model significantly.

IV. CONCLUSIONS

We investigated R^p inflation with $p \approx 2$ in order to evaluate deviations from R^2 inflation. Using the inflaton potential in the Einstein frame, we explicitly wrote down the scalar spectral index n_s , its running α , and the tensor-to-scalar ratio r as in (33), which are presented in Fig. 3. We can also explicitly draw the consistency relation as presented in Fig. 4. We showed that the parameter region $p \gtrsim 1.95$ is solely constrained by n_s and a precise measurement of (n_s, r) or (r, α) can test a whole range of p . Specifically, for $N_k = 60$, $r \leq 0.05$ requires $1.92 \lesssim p \leq 2$ and $0.96 \lesssim n_s \lesssim 0.99$, while $0.05 \leq r \leq 0.1$ requires $1.88 \lesssim p \lesssim 1.92$ and $0.98 \lesssim n_s \lesssim 0.99$. On the other hand, for fixed $n_s = 0.96$, $r \simeq 0.05$ and 0.1 require $(p, N_k) \simeq (1.93, 30)$ and $(1.9, 27)$, respectively.

ACKNOWLEDGMENTS

We thank W. Hu and A. A. Starobinsky for useful discussions. This work was supported by Japan Society for the Promotion of Science Postdoctoral Fellowships for Research Abroad.

-
- [1] A. A. Starobinsky, Phys.Lett. **B91**, 99 (1980).
 - [2] A. Vilenkin, Phys.Rev. **D32**, 2511 (1985).
 - [3] M. B. Mijic, M. S. Morris, and W.-M. Suen, Phys.Rev. **D34**, 2934 (1986).
 - [4] L. Ford, Phys.Rev. **D35**, 2955 (1987).
 - [5] G. Hinshaw *et al.* (WMAP), Astrophys.J.Suppl. **208**, 19 (2013), arXiv:1212.5226 [astro-ph.CO].
 - [6] P. Ade *et al.* (Planck Collaboration), (2013), arXiv:1303.5082 [astro-ph.CO].
 - [7] P. Ade *et al.* (BICEP2 Collaboration), Phys.Rev.Lett. **112**, 241101 (2014), arXiv:1403.3985 [astro-ph.CO].
 - [8] R. Adam *et al.* (Planck Collaboration), (2014), arXiv:1409.5738 [astro-ph.CO].
 - [9] W. Hu and I. Sawicki, Phys.Rev. **D76**, 064004 (2007), arXiv:0705.1158 [astro-ph].
 - [10] S. A. Appleby and R. A. Battye, Phys.Lett. **B654**, 7 (2007), arXiv:0705.3199 [astro-ph].
 - [11] A. A. Starobinsky, JETP Lett. **86**, 157 (2007), arXiv:0706.2041 [astro-ph].
 - [12] H. Motohashi, A. A. Starobinsky, and J. Yokoyama, Prog.Theor.Phys. **123**, 887 (2010), arXiv:1002.1141 [astro-ph.CO].
 - [13] H. Motohashi, A. A. Starobinsky, and J. Yokoyama, JCAP **1106**, 006 (2011), arXiv:1101.0744 [astro-ph.CO].
 - [14] R. Gannouji, B. Moraes, and D. Polarski, JCAP **0902**, 034 (2009), arXiv:0809.3374 [astro-ph].
 - [15] H. Motohashi, A. A. Starobinsky, and J. Yokoyama, Int.J.Mod.Phys. **D18**, 1731 (2009), arXiv:0905.0730 [astro-ph.CO].
 - [16] S. Tsujikawa, R. Gannouji, B. Moraes, and D. Polarski, Phys.Rev. **D80**, 084044 (2009), arXiv:0908.2669 [astro-ph.CO].
 - [17] H. Motohashi, A. A. Starobinsky, and J. Yokoyama, Prog.Theor.Phys. **124**, 541 (2010), arXiv:1005.1171 [astro-ph.CO].
 - [18] H. Motohashi, A. A. Starobinsky, and J. Yokoyama, Phys.Rev.Lett. **110**, 121302 (2013), arXiv:1203.6828 [astro-ph.CO].
 - [19] S. Tsujikawa, Phys.Rev. **D77**, 023507 (2008), arXiv:0709.1391 [astro-ph].
 - [20] S. Appleby and R. Battye, JCAP **0805**, 019 (2008), arXiv:0803.1081 [astro-ph].
 - [21] A. V. Frolov, Phys.Rev.Lett. **101**, 061103 (2008), arXiv:0803.2500 [astro-ph].
 - [22] T. Kobayashi and K.-i. Maeda, Phys.Rev. **D78**, 064019 (2008), arXiv:0807.2503 [astro-ph].
 - [23] S. A. Appleby, R. A. Battye, and A. A. Starobinsky, JCAP **1006**, 005 (2010), arXiv:0909.1737 [astro-ph.CO].
 - [24] H. Motohashi and A. Nishizawa, Phys.Rev. **D86**, 083514 (2012), arXiv:1204.1472 [astro-ph.CO].
 - [25] A. Nishizawa and H. Motohashi, Phys.Rev. **D89**, 063541 (2014), arXiv:1401.1023 [astro-ph.CO].
 - [26] H. Schmidt, Class.Quant.Grav. **6**, 557 (1989).
 - [27] K.-i. Maeda, Phys.Rev. **D39**, 3159 (1989).
 - [28] V. Muller, H. Schmidt, and A. A. Starobinsky, Class.Quant.Grav. **7**, 1163 (1990).
 - [29] S. Gottlober, V. Muller, H. Schmidt, and A. A. Starobinsky, Int.J.Mod.Phys. **D1**, 257 (1992).
 - [30] A. De Felice and S. Tsujikawa, Living Rev.Rel. **13**, 3 (2010), arXiv:1002.4928 [gr-qc].

- [31] J. Martin, C. Ringeval, and V. Vennin, *Phys.Dark Univ.* (2014), 10.1016/j.dark.2014.01.003, arXiv:1303.3787 [astro-ph.CO].
- [32] J. Martin, C. Ringeval, R. Trotta, and V. Vennin, *JCAP* **1403**, 039 (2014), arXiv:1312.3529 [astro-ph.CO].
- [33] A. Codello, J. Joergensen, F. Sannino, and O. Svendsen, *JHEP* **1502**, 050 (2015), arXiv:1404.3558 [hep-ph].
- [34] J. Martin, C. Ringeval, R. Trotta, and V. Vennin, *Phys.Rev.* **D90**, 063501 (2014), arXiv:1405.7272 [astro-ph.CO].
- [35] M. Artymowski and Z. Lalak, *JCAP* **1409**, 036 (2014), arXiv:1405.7818 [hep-th].
- [36] I. Ben-Dayan, S. Jing, M. Torabian, A. Westphal, and L. Zarate, *JCAP* **1409**, 005 (2014), arXiv:1404.7349 [hep-th].
- [37] M. Rinaldi, G. Cognola, L. Vanzo, and S. Zerbini, *JCAP* **1408**, 015 (2014), arXiv:1406.1096 [gr-qc].
- [38] M. Rinaldi, G. Cognola, L. Vanzo, and S. Zerbini, (2014), arXiv:1410.0631 [gr-qc].
- [39] R. Costa and H. Nastase, *JHEP* **1406**, 145 (2014), arXiv:1403.7157 [hep-th].
- [40] G. K. Chakravarty and S. Mohanty, (2014), arXiv:1405.1321 [hep-ph].
- [41] T. Chiba and M. Yamaguchi, *JCAP* **0810**, 021 (2008), arXiv:0807.4965 [astro-ph].
- [42] J.-O. Gong, J.-c. Hwang, W.-I. Park, M. Sasaki, and Y.-S. Song, *JCAP* **1109**, 023 (2011), arXiv:1107.1840 [gr-qc].
- [43] H. Motohashi and W. Hu, (2015), arXiv:1503.04810 [astro-ph.CO].